Conclusion

Some tentative examples have been presented to illustrate the need for global understanding of the potential surface. Although the Teller theorem is well-known, its implications have not been carefully considered previously. The network of branch-cuts is a topological feature which must be carefully considered in a global discussion of polyatomic potential surfaces because the existence of such a network to a certain extent invalidates the adiabatic approximation for describing nuclear motion. Because of the possibility of sign-reversing loops which lie at a great distance from branch-cut singularities, it is generally impossible to assign an electronic wave function to each nuclear configuration in such a way that the wave function is continuous in nuclear coordinates.

Acknowledgment. The author is grateful to Charles F. Bender and Lawrence Livermore Laboratory for calculations on CH_2. This research was supported by the National Science Foundation.

References and Notes

(1) D. R. Bates, K. Ledsham, and A. L. Stewart, *Phil. Trans. R. Soc. London, Ser. A*, **246**, 215 (1953).
(2) F. Hund, *Z. Phys.*, **40**, 742 (1927).
(3) J. C. Slater, *J. Chem. Phys.*, **41**, 3199 (1964).
(4) A. D. Walsh, *J. Chem. Soc.*, 2260 (1953).
(5) R. J. Buenker and S. D. Peyerimhoff, *Chem. Rev.*, **74**, 127 (1974).
(6) J. N. Murrell and K. J. Laidler, *Trans. Faraday Soc.*, **64**, 371 (1968).
(7) J. N. Murrell and G. L. Pratt, *Trans. Faraday Soc.*, **66**, 1680 (1970).
(8) E. Teller, *J. Phys. Chem.*, **41**, 109 (1937).
(9) E. E. Nikitin, *Adv. Chem. Phys.*, **28**, 317 (1975), and references therein.
(10) H. A. Jahn and E. Teller, *Proc. R. Soc. London, Ser. A*, **161**, 220 (1937).
(11) C. F. Jackels and E. R. Davidson, *J. Chem. Phys.*, **64**, 2908 (1976).
(12) H. C. Longuet-Higgins, *Proc. R. Soc. London, Ser. A*, **344**, 147 (1975).
(13) K. R. Naqvi and W. B. Brown, *Int. J. Quantum Chem.*, **6**, 271 (1972); K. R. Naqvi, *Chem. Phys. Lett.*, **15**, 634 (1972); G. J. Hoytink, *ibid.*, **34**, 414 (1975), have recently criticized this proof as well as the simpler dimensionality proof of J. V. Neumann and E. P. Wigner, *Z. Phys.*, **30**, 467 (1929), and the examples given by G. H. Herzberg and H. C. Longuet-Higgins, *Discuss. Faraday Soc.*, **No. 35**, 77 (1963). As pointed out by Longuet-Higgins in ref 12, these criticisms are invalid because they miss the point of the original proofs. The phrase "usually not happen" in the text refers to the fact that the family of hamiltonians for which ξ_2 and ξ_3 are linearly dependent is a set of measure zero in the family of all hamiltonians which can be constructed.
(14) B. Liu, *J. Chem. Phys.*, **58**, 1925 (1973).
(15) R. N. Porter, R. M. Stevens, and M. Karplus, *J. Chem. Phys.*, **49**, 5163 (1968).
(16) J. W. C. Johns, S. H. Priddle, and D. A. Ramsey, *Discuss. Faraday Soc.*, **No. 35**, 90 (1963).
(17) R. Renner, *Z. Phys.*, **92**, 172 (1934).

Synthesis, Structure, and Bonding of the Tetrameric Cyclopentadienyliron Sulfide Monocation, $[Fe_4(\eta^5\text{-}C_5H_5)_4(\mu_3\text{-}S)_4]^+$: Stereochemical Consequences Due to Oxidation of a Cubane-Like Fe_4S_4 Core[1]

Trinh-Toan, W. Peter Fehlhammer, and Lawrence F. Dahl*[2]

Contribution from the Department of Chemistry, University of Wisconsin, Madison, Wisconsin 53706. *Received June 16, 1976*

Abstract: The $[Fe_4(\eta^5\text{-}C_5H_5)_4(\mu_3\text{-}S)_4]^+$ monocation was obtained from oxidation of the neutral $Fe_4(\eta^5\text{-}C_5H_5)_4(\mu_3\text{-}S)_4$ cluster by different oxidizing agents such as $AgBF_4$, I_2, and Br_2. An x-ray diffraction study of the $[Fe_4(\eta^5\text{-}C_5H_5)_4(\mu_3\text{-}S)_4]Br$ salt reveals that the one-electron oxidation of the neutral species distorts the Fe_4S_4 core from a tetragonal D_{2d}-$\bar{4}2m$ geometry containing two electron-pair bonding and four nonbonding Fe–Fe distances of 2.64 and 3.36 Å, respectively, to an orthorhombic D_2-222 geometry possessing three pairs of Fe–Fe distances of 2.65, 3.19, and 3.32 Å. This preferential shortening of *two* of the *four* long Fe–Fe distances in the monocation relative to those in the parent molecule is attributed to the removal of an electron from an antibonding iron cluster orbital of degenerate e representation (under D_{2d} symmetry), which thereby produces the observed orthorhombic distortion via a first-order Jahn–Teller effect. Crystals of $[Fe_4(\eta^5\text{-}C_5H_5)_4(\mu_3\text{-}S)_4]Br$ are monoclinic with space group symmetry $A2/a$ and lattice constants a = 15.668 (2) Å, b = 13.289 (2) Å, c = 13.996 (2) Å, β = 124.48 (1)°, and ρ_{obsd} = 1.94 vs. ρ_{calcd} = 1.91 g cm^{-3} for Z = 4. Least-squares refinement gave R_1 = 8.0% and R_2 = 7.1% for 1053 independent diffractometry data with $I \geq 2.0\sigma(I)$.

As part of an extensive examination of the influence of valence electrons on the geometries of various classes of ligand-bridged metal clusters via oxidation and/or reduction of the neutral species, we have concentrated upon the synthesis and structural characterization of cubane-like metal clusters containing four transition metal atoms and four triply bridging ligands at the alternate apices of a distorted cube.[3,4]

Our preparation of the $[Fe_4(\eta^5\text{-}C_5H_5)_4(\mu_3\text{-}S)_4]^+$ monocation by oxidation of the diamagnetic neutral tetramer together with its structural determination was a consequence not only of its importance from theoretical considerations but also of its possible biological implications (during the time of its synthesis by us[1] and independently by Ferguson and Meyer[5]) in that the neutral parent[6] was then proposed[7] to be a possible model for the redox center of the reduced form of the high-potential iron protein isolated from the photosynthetic bacterium *Chromatium*.[8-10] The fact that this paramagnetic $[Fe_4(\eta^5\text{-}C_5H_5)_4(\mu_4\text{-}S)_4]^+$ monocation possessed a hitherto unknown molecular orbital electronic configuration for a cubane-like species made it especially desirable to determine the stereochemical effect of a one-electron oxidation on the Fe_4S_4 core. The resulting structural information presented here has provided a requisite basis for our subsequent studies[4] directed toward a systematization of the topological nature of cubane-like transition metal clusters from which the geometries of such complexes can be correlated with the varying number of electrons in the metal cluster orbitals.

Experimental Section

Preparation and Properties. (a) General Remarks. The neutral $Fe_4(\eta^5\text{-}C_5H_5)_4(\mu_3\text{-}S)_4$ complex was prepared as described previously.[6b] The cationic species was obtained in nearly quantitative yields from oxidation of $Fe_4(\eta^5\text{-}C_5H_5)_4(\mu_3\text{-}S)_4$ by different oxidizing agents such as $AgBF_4$, I_2, and Br_2. The $[Fe_4(\eta^5\text{-}C_5H_5)_4(\mu_3\text{-}S)_4][PF_6]$ salt

was produced by Ferguson and Meyer[5] by controlled potential electrolysis of the neutral molecule. The treatment of solvents and the reaction conditions have been described previously.[3]

(b) Preparation of $[Fe_4(\eta^5\text{-}C_5H_5)_4(\mu_3\text{-}S)_4]Br_3$. A mixture of bromine and CH_2Cl_2 (1:10) was added dropwise to a stirred solution of $Fe_4(\eta^5\text{-}C_5H_5)_4(\mu_3\text{-}S)_4$ in CH_2Cl_2 until the originally dark brown solution turned to pale yellow, showing an excess of bromine. The almost black precipitate of $[Fe_4(\eta^5\text{-}C_5H_5)_4(\mu_3\text{-}S)_4]Br_3$ was filtered off, repeatedly washed with CH_2Cl_2–ether mixture, and crystallized from nitromethane.

Anal. Calcd for $C_{20}H_{20}Br_3Fe_4S_4$: C, 28.20; H, 2.37; Fe, 26.23; Br, 28.15. Found:[11] C, 28.24; H, 2.10; Fe, 26.86; Br, 28.63.

(c) Preparation of $[Fe_4(\eta^5\text{-}C_5H_5)_4(\mu_3\text{-}S)_4]Br$. Crude $[Fe_4(\eta^5\text{-}C_5H_5)_4(\mu_3\text{-}S)_4]Br_3$ was extracted on a Soxhlet apparatus with methanol for 3–4 days. After this period crystals of $[Fe_4(\eta^5\text{-}C_5H_5)_4(\mu_3\text{-}S)_4]Br$ were deposited on the wall of the slowly cooled reaction flask. It is probable that continuous boiling in methanol is the cause of the decomposition of the tribromide anions into bromide anions.

Anal. Calcd for $C_{20}H_{20}BrFe_4S_4$: C, 34.72; H, 2.91; Fe, 32.28; Br, 11.55. Found: C, 34.88; H, 3.36; Fe, 29.69; Br, 12.25.

The infrared spectrum of $[Fe_4(\eta^5\text{-}C_5H_5)_4(\mu_3\text{-}S)_4]Br$ as a KBr pellet shows absorption bands at 3080 (w), 3010 (w), 1820 (w), 1635 (m), 1415 (w), 850 (br), and 820 (br) cm^{-1} characteristic of the η^5- cyclopentadienyl rings.

(d) Preparation of $[Fe_4(\eta^5\text{-}C_5H_5)_4(\mu_3\text{-}S)_4]I_4$. The procedure of preparation closely followed that outlined for the bromide salts. Excessive iodine dissolved in CH_2Cl_2 was allowed to react with a dilute solution of $Fe_4(\eta^5\text{-}C_5H_5)_4(\mu_3\text{-}S)_4$ in CH_2Cl_2 for 1–2 h, whereby a dark brown solid separated. Small crystals of the metal cluster salt were obtained by methanol extraction in an almost quantitative yield. Extraction with acetone resulted in partial decomposition of the compound.

Anal. Calcd for $C_{20}H_{20}Fe_4I_4S_4$: C, 21.46; H, 1.80; Fe, 19.95; I, 45.34. Found: C, 21.21; H, 1.79; Fe, 19.78; I, 45.60.

The ratio of four iodine atoms per tetrameric monocation suggests that there may be two kinds of anions in the crystal such as either an I_3^-–I_5^- or an I^-–I_7^- combination.

(e) Preparation of $[Fe_4(\eta^5\text{-}C_5H_5)_4(\mu_3\text{-}S)_4]BF_4$. This preparation was carried out in a dry nitrogen atmosphere. Equimolar amounts of $AgBF_4$ in CH_2Cl_2 were added under vigorous stirring to a dilute solution of $Fe_4(\eta^5\text{-}C_5H_5)_4(\mu_3\text{-}S)_4$ in CH_2Cl_2 whereby a black precipitate was formed. The crude product was then transferred to a thimble and extracted with ethanol. The salt was subsequently recrystallized in CH_3CN to yield black shiny crystals.

Crystal Data for $[Fe_4(\eta^5\text{-}C_5H_5)_4(\mu_3\text{-}S)_4]Br$. Of the prepared salts, only the tetraiodide and the bromide ones were recrystallized under our experimental conditions to yield single crystals of sizes suitable for x-ray diffraction studies. The $[Fe_4(\eta^5\text{-}C_5H_5)_4(\mu_3\text{-}S)_4]Br$ compound was selected for the structural determination.

A prism-shaped crystal of approximate size $0.14 \times 0.14 \times 0.25$ mm with well-developed $\{011\}$ faces and slanted $\{21\bar{1}\}$ faces at the ends of the prism was used for the collection of intensity data.

Preliminary Weissenberg and precession photographs showed monoclinic C_{2h}-$2/m$ Laue symmetry. Subsequently, the crystal was optically aligned about the a rotation axis on a Datex-controlled General Electric diffractometer equipped with an E&A full circle and then centered in the x-ray beam. The alignment procedure has been described previously.[12,13] Intensity data were collected for $2\theta \leq 42°$ with Zr-filtered Mo Kα radiation at a takeoff angle of 2.0°. Intensities were recorded by the θ–2θ scan method at a 2.0°/min rate with (stationary crystal)–(stationary counter) background counts of 15 s taken on each side of the scan. The treatment of intensity data including corrections for background and Lorentz-polarization effects has been given previously.[14] Since calculated transmission coefficients,[13c] based on a linear absorption coefficient[15a] for Mo Kα radiation of 45.2 cm^{-1}, ranged only from 0.54 to 0.62, absorption corrections of the intensities were neglected. Of the total of 1354 independent reflections, the 1053 reflections for which $I \geq 2.0\sigma(I)$ were used in the solution and refinement of the structure.

The $[Fe_4(\eta^5\text{-}C_5H_5)_4(\mu_3\text{-}S)_4]Br$ salt crystallizes in a monoclinic unit cell of dimensions $a = 15.668$ (2) Å, $b = 13.289$ (2) Å, $c = 13.996$ (2) Å, and $\beta = 124.48$ (1)°; the cell volume is 2402.3 Å^3. The observed density of 1.94 g cm^{-3} (flotation method) is in accord with the calculated value of 1.91 g cm^{-3} based on four formula species per unit cell. The total number of electrons per unit cell, $F(000)$, is 1372.

Systematic absences of $\{hkl\}$ for $k + l$ odd and of $\{h0l\}$ for h odd denote the probable space groups as either Aa (nonstandard setting of Cc (C_s^4, No. 9), b axis unique) or $A2/a$ (nonstandard setting of $C2/c$ (C_{2h}^8, No. 15), b axis unique). The successful refinement justified the choice of the latter centrosymmetric space group. In the $A2/a$ cell the four bromide anions and the centers of the four cations are situated on crystallographic twofold axes. For this centrosymmetric space group each of the crystallograpically independent atoms of the $[Fe_4(\eta^5\text{-}C_5H_5)_4(\mu_3\text{-}S)_4]^+$ monocation occupies the eightfold set of general positions $8f$: $(0, 0,0; 0,\frac{1}{2},\frac{1}{2}) \pm (x,y,z; \frac{1}{2}+x,\bar{y},z)$, while the bromide anions occupy the fourfold set of special positions $4e$: $(0,0,0; 0,\frac{1}{2},\frac{1}{2}) \pm (\frac{1}{4},y,\frac{1}{2})$.

Determination and Refinement of the Structure. Initial coordinates for the one independent bromine and two independent iron atoms were obtained from a three-dimensional sharpened Patterson function, and two Fourier syntheses coupled with one cycle of isotropic least-squares refinement revealed the positions of all nonhydrogen atoms. Full-matrix refinement with individual isotropic thermal parameters for all 15 nonhydrogen atoms led to convergence at $R_1 = 11.4\%$ and $R_2 = 14.4\%$.[16,17] Further refinement was carried out with anisotropic thermal parameters utilized for all nonhydrogen atoms together with the inclusion of cyclopentadienyl hydrogen atoms for which isotropic temperature factors were assigned and new idealized positions were calculated[3,13g] after each cycle and then included in the structure factor calculations of the next cycle as fixed-atom contributions. Convergence was reached at $R_1 = 8.0\%$ and $R_2 = 7.1\%$. During the last cycle no positional parameters changed by more than 0.3σ and no thermal parameters shifted by more than 0.4σ. A final difference Fourier synthesis was virtually featureless.

The positional and thermal parameters obtained from the output of the last cycle of least-squares refinement are presented in Table I. Interatomic distances and bond angles along with esd's, calculated from the full inverse matrix, are listed in Table II. Equations of the mean planes[13h] for the cyclopentadienyl rings, together with out-of-plane distances of atoms and dihedral angles between these planes are tabulated elsewhere along with the observed and calculated structure factors; see paragraph at end of paper regarding supplementary material.

Results and Discussion

Description of the Crystal Structure. Crystalline $[Fe_4(\eta^5\text{-}C_5H_5)_4(\mu_3\text{-}S)_4]Br$ is constructed of discrete $[Fe_4(\eta^5\text{-}C_5H_5)_4(\mu_3\text{-}S)_4]^+$ cations and Br^- anions. Figure 1 displays the architecture of one $[Fe_4(\eta^5\text{-}C_5H_5)_4(\mu_3\text{-}S)_4]^+$ monocation of crystallographic site symmetry C_2-2. Its Fe_4S_4 framework is sufficiently embodied within the four cyclopentadienyl rings such that there are no interionic van der Waals contacts to the sulfur atoms. The crystal packing appears to be determined largely by Br···H interactions as indicated by four H···Br distances of 2.7–3.1 Å (Table II) which are shorter than the van der Waals separation of 3.15 Å.[18] All interionic H···H distances are longer than the van der Waals contact of 2.4 Å[18] except for one contact of 2.3 Å. The arrangement of the cations and anions in the monoclinic unit cell is shown in Figure 2.

The $[Fe_4(\eta^5\text{-}C_5H_5)_4(\mu_3\text{-}S)_4]^+$ Monocation. The structural determination shows that the monocation retains the overall cubane-like Fe_4S_4 framework of the neutral homologue with the triply bridging sulfur atoms situated above the four triangular faces of the iron tetrahedron. Figure 3 exhibits the local environment of the two crystallographically independent iron atoms showing their chemical equivalence in each not only being bonded to a η^5-cyclopentadienyl ring and three triply bridging sulfur atoms but also being involved in different degrees of interaction with the other three iron atoms.

The salient structural feature of the monocation is that the Fe_4S_4 core experimentally conforms to an orthorhombic D_2-222 geometry. The six Fe–Fe distances (of which four are crystallographically independent) separate under this symmetry into one pair of lengths 2.643 (4) and 2.661 (5) Å, a second pair of identical length 3.188 (3) Å, and a third pair of identical length 3.319 (3) Å. The close conformity of the entire Fe_4S_4 core to orthorhombic D_2 symmetry is shown by: (1) the

Table I. Positional and Thermal Parameters with Estimated Standard Deviations[a]

Atom	x	y	z	B (Å^2)
Br	0.2500	0.0664 (2)	0.5000	*b*
Fe(1)	0.2650 (2)	0.1653 (2)	0.1035 (2)	*b*
Fe(2)	0.3523 (2)	−0.0348 (2)	0.0625 (2)	*b*
S(1)	0.2549 (3)	−0.0009 (3)	0.1242 (4)	*b*
S(2)	0.3800 (3)	0.1314 (3)	0.0664 (4)	*b*
C(1)	0.2466 (21)	0.3244 (14)	0.1284 (19)	*b*
C(2)	0.3470 (18)	0.2971 (20)	0.1987 (23)	*b*
C(3)	0.3614 (17)	0.2177 (22)	0.2733 (20)	*b*
C(4)	0.2625 (24)	0.1952 (15)	0.2489 (20)	*b*
C(5)	0.1886 (15)	0.2616 (18)	0.1570 (21)	*b*
C(6)	0.3894 (20)	−0.1890 (20)	0.0636 (47)	*b*
C(7)	0.4164 (38)	−0.1595 (40)	0.1730 (49)	*b*
C(8)	0.4866 (31)	−0.0889 (32)	0.2097 (25)	*b*
C(9)	0.5025 (20)	−0.0753 (19)	0.1209 (49)	*b*
C(10)	0.4462 (28)	−0.1341 (28)	0.0378 (23)	*b*
H(1)	0.2188	0.3837	0.0635	5.0[d]
H(2)	0.4077	0.3338	0.1958	5.0
H(3)	0.4344	0.1810	0.3370	5.0
H(4)	0.2465	0.1379	0.2925	5.0
H(5)	0.1054	0.2639	0.1170	5.0
H(6)	0.3329	−0.2460	0.0072	5.0
H(7)	0.3870	−0.1874	0.2224	5.0
H(8)	0.5228	−0.0510	0.2931	5.0
H(9)	0.5543	−0.0235	0.1168	5.0
H(10)	0.4467	−0.1367	−0.0398	5.0

	Thermal Coefficients					
Atom	β_{11}	β_{22}	β_{33}	β_{12}	β_{13}	β_{23}
Br	852 (23)	553 (22)	1235 (35)	0[c]	463 (25)	0[c]
Fe(1)	549 (18)	546 (19)	673 (27)	−54 (14)	356 (19)	−57 (18)
Fe(2)	464 (16)	478 (18)	697 (28)	1 (13)	291 (18)	34 (17)
S(1)	551 (31)	496 (32)	624 (50)	30 (25)	312 (34)	8 (32)
S(2)	432 (31)	449 (31)	735 (51)	−23 (24)	296 (34)	−60 (30)
C(1)	1284 (219)	503 (146)	1553 (297)	25 (154)	1001 (242)	−151 (168)
C(2)	792 (191)	1041 (214)	1205 (286)	−179 (168)	548 (206)	−520 (198)
C(3)	797 (188)	1453 (264)	855 (257)	271 (195)	227 (186)	−284 (215)
C(4)	1711 (263)	651 (158)	810 (226)	55 (182)	760 (215)	−73 (159)
C(5)	1068 (182)	813 (173)	1678 (318)	−189 (163)	1061 (228)	−683 (191)
C(6)	261 (153)	228 (157)	3824 (699)	21 (114)	−70 (286)	1 (286)
C(7)	1457 (365)	1402 (396)	2327 (539)	948 (284)	1176 (416)	1525 (414)
C(8)	1133 (280)	1349 (353)	745 (265)	657 (227)	−31 (228)	−559 (255)
C(9)	521 (174)	518 (177)	2902 (523)	189 (137)	890 (286)	233 (269)
C(10)	980 (240)	784 (224)	1208 (302)	333 (175)	48 (240)	−125 (219)

[a] In this and the following tables, estimated standard deviations are given in parentheses. [b] Anisotropic temperature factors of the form $\exp\{-(\beta_{11}h^2 + \beta_{22}k^2 + \beta_{33}l^2 + 2\beta_{12}hk + 2\beta_{13}hl + 2\beta_{23}kl)\}$ were used for the bromine, iron, sulfur, and carbon atoms. The resulting thermal coefficients ($\times 10^5$) are as shown. [c] The location of Br on a twofold rotation axis in the *b*-direction requires the anisotropic thermal coefficients β_{12} and β_{23} to be zero by symmetry. [d] Hydrogen atoms were each assigned isotropic thermal parameters of B = 5.0 Å^2.

nonbonding tetrahedron of sulfur atoms also dividing into three distinct pairs with one pair of identical length 2.879 (6) Å, another pair of identical length 3.062 (6) Å, and the third pair of chemically equivalent lengths 3.387 (7) and 3.391 (9) Å; (2) the 12 Fe–S bond lengths (of which six are independent) separating into three sets with mean values 2.185, 2.212, and 2.246 Å; (3) the 12 Fe–S–Fe bond angles (with six being independent) splitting into three distinct sets of averages 74.2, 92.1, and 96.3°; and (4) the six crystallographically independent S–Fe–S bond angles likewise breaking down into three distinguishable pairs of averages 80.5, 87.5, and 100.9°

Electronic Influence of the Fe–Fe Bonding. Comparison of $[Fe_4(\eta^5\text{-}C_5H_5)_4(\mu_3\text{-}S)_4]^+$ Monocation with $Fe_4(\eta^5\text{-}C_5H_5)_4(\mu_3\text{-}S)_4$ Molecule. Of prime interest is a comparison of the geometries of the neutral and monocharged species. Previous structural characterization by x-ray diffraction of the parent molecule, crystallized in both a monoclinic[6b] and orthorhombic[6a] crystalline phase, established its tetragonal D_{2d}-$\bar{4}2m$ geometry to be essentially invariant to crystal packing. The Fe_4S_4 framework in the monoclinic (orthorhombic) phase is elongated along the S_4-$\bar{4}$ axis to give for the iron tetrahedron two electron-pair bonding distances of 2.65 (2.63) Å and four nonbonding distances of 3.36 (3.37) Å. In the monocation one of the electron-pair Fe–Fe bonds is rotated about the principal S_4-$\bar{4}$ axis by 7° from perpendicularity relative to the other electron-pair Fe–Fe bond such that the idealized D_{2d} geometry of the neutral molecule is reduced to an idealized D_2 geometry. This angular deformation in the monocation relative to its parent molecule is due to a much larger decrease by 0.17 Å of two nonbonding Fe–Fe distances compared to a decrease of 0.04 Å for the other two nonbonding Fe–Fe distances. On the other hand, the two electron-pair Fe–Fe distances of 2.65 Å in the monocation remain essentially unaltered from the corresponding distances in the neutral tetramer.

This preferential shortening of *two* of the *four* long Fe–Fe distances in the monocation relative to those in the neutral molecule expectedly gives rise to significant changes in other distances and bond angles of the Fe_4S_4 framework. A pictorial

Table II. Interatomic Distances and Bond Angles

A. Intramolecular Distances (Å)			
Fe(1)-Fe(1')[a]	2.661 (5)	S(1)···S(1')	3.391 (9)
Fe(2)-Fe(2')	2.643 (4)	S(2)···S(2')	3.387 (7)
Fe(1)-Fe(2)	3.188 (3)	S(1)···S(2)	3.062 (6)
Fe(1)···Fe(2')	3.319 (3)	S(1)···S(2')	2.879 (6)
Fe(1)-S(1)	2.245 (5)	Fe(2)-S(1)	2.183 (5)
Fe(1)-S(2)	2.186 (5)	Fe(2)-S(2)	2.246 (5)
Fe(1)-S(2')	2.214 (5)	Fe(2)-S(1')	2.210 (5)
Fe(1)-C(1)	2.19 (2)	Fe(2)-C(6)	2.13 (2)
Fe(1)-C(2)	2.13 (2)	Fe(2)-C(7)	2.09 (3)
Fe(1)-C(3)	2.08 (2)	Fe(2)-C(8)	2.07 (2)
Fe(1)-C(4)	2.09 (2)	Fe(2)-C(9)	2.08 (2)
Fe(1)-C(5)	2.15 (2)	Fe(2)-C(10)	2.15 (2)
C(1)-C(2)	1.35 (2)	C(6)-C(7)	1.40 (4)
C(2)-C(3)	1.41 (3)	C(7)-C(8)	1.31 (4)
C(3)-C(4)	1.42 (3)	C(8)-C(9)	1.41 (4)
C(4)-C(5)	1.45 (3)	C(9)-C(10)	1.26 (3)
C(5)-C(1)	1.45 (2)	C(10)-C(6)	1.35 (4)
B. Closest Nonbonding Intermolecular Distances (Å)			
Br···H(4)	3.03	S(2)···H(10)[e]	2.94
Br···H(6)[b,c]	2.79		
Br···H(1)[b,c]	2.72	H(5)···H(7)[e]	2.28
Br···H(8)[d,e]	3.07	H(9)···H(10)[e]	2.38
C. Bond Angles (deg)			
S(1)-Fe(1)-S(2)	87.4 (2)	S(1)-Fe(2)-S(2)	87.5 (2)
S(1)-Fe(1)-S(2')	80.4 (2)	S(1)-Fe(2)-S(1')	101.1 (2)
S(2)-Fe(1)-S(2')	100.7 (2)	S(2)-Fe(2)-S(1')	80.5 (2)
Fe(1)-S(1)-Fe(2)	92.1 (2)	Fe(1)-S(2)-Fe(2)	92.0 (2)
Fe(1)-S(1)-Fe(2')	96.3 (2)	Fe(1)-S(2)-Fe(1')	74.4 (2)
Fe(2)-S(1)-Fe(2')	74.0 (2)	Fe(2)-S(2)-Fe(1')	96.2 (2)
Fe(1')-Fe(1)-S(1)	99.1 (1)	Fe(2')-Fe(2)-S(1)	53.5 (1)
Fe(1')-Fe(1)-S(2)	52.3 (1)	Fe(2')-Fe(2)-S(2)	99.3 (1)
Fe(1')-Fe(1)-S(2')	52.3 (1)	Fe(2')-Fe(2)-S(1')	52.5 (1)
C(1)-C(2)-C(3)	111.9 (21)	C(6)-C(7)-C(8)	107.3 (33)
C(2)-C(3)-C(4)	106.6 (19)	C(7)-C(8)-C(9)	105.9 (28)
C(3)-C(4)-C(5)	107.5 (19)	C(8)-C(9)-C(10)	110.8 (26)
C(4)-C(5)-C(1)	106.6 (17)	C(9)-C(10)-C(6)	108.2 (30)
C(5)-C(1)-C(2)	107.4 (19)	C(10)-C(6)-C(7)	107.7 (28)

[a] Atoms in the prime set are related to unprime atoms by the crystallographic twofold axis located at $x = \frac{1}{4}, z = 0$. Hydrogen atoms with superscripts from b to e are related to the unprime ones by the following operations: [b] $x, \frac{1}{2}+y, \frac{1}{2}+z$; [c] $\frac{1}{2}-x, \frac{1}{2}+y, \frac{1}{2}-z$; [d] $\frac{1}{2}+x, -y, z$; [e] $-x, -y, -z$.

description of the molecular distortion of the monocation from the neutral reduced species is illustrated in Figure 4.

The stereochemical effects imposed on the η^5-cyclopentadienyl rings of the monocation are not unusual. The observed C-C distances (Table II) are analogous to those determined by x-ray diffraction of other cubane-like metal cyclopentadienyl complexes.[3,4a,6,19] The cyclopentadienyl carbon atoms are coplanar within 0.006 Å in one ring and within 0.003 Å in the other independent ring. Furthermore, the mean Fe-C_5H_5 (centroid) distance of 1.76 Å in the monocation is unchanged from the corresponding distance observed in the neutral $Fe_4(\eta^5\text{-}C_5H_5)_4(\mu_3\text{-}S)_4$.

Bonding Description of the $[Fe_4(\eta^5\text{-}C_5H_5)_4(\mu_3\text{-}S)_4]^n$ Clusters ($n = 0, +1$). A molecular orbital approach is necessary in order to rationalize the observed differences in the geometries of the monocationic and neutral species. Since a qualitative MO formulation of the bonding has been developed elsewhere[20] for $Fe_4(\eta^5\text{-}C_5H_5)_4(\mu_3\text{-}S)_4$, only its main features are outlined here. Through coordination with the cyclopentadienyl and sulfide anions each iron atom in the $Fe_4(\eta^5\text{-}C_5H_5)_4(\mu_3\text{-}S)_4$ molecule

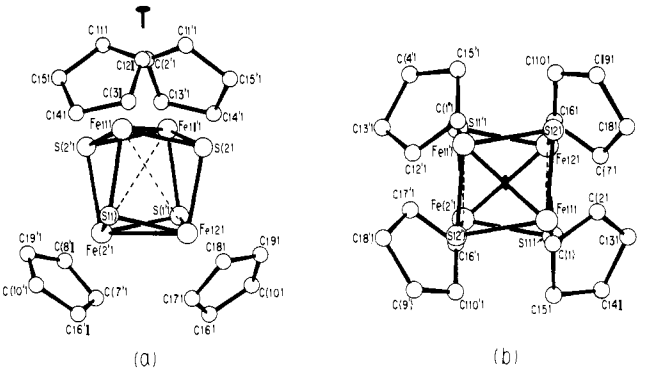

Figure 1. (a) A general view and the atomic numbering scheme of the $[Fe_4(\eta^5\text{-}C_5H_5)_4(\mu_3\text{-}S)_4]^+$ monocation. The dashed lines represent weak Fe-Fe interactions of bond order less than one. Ring hydrogen atoms are not shown; (b) a view down the crystallographic twofold axis.

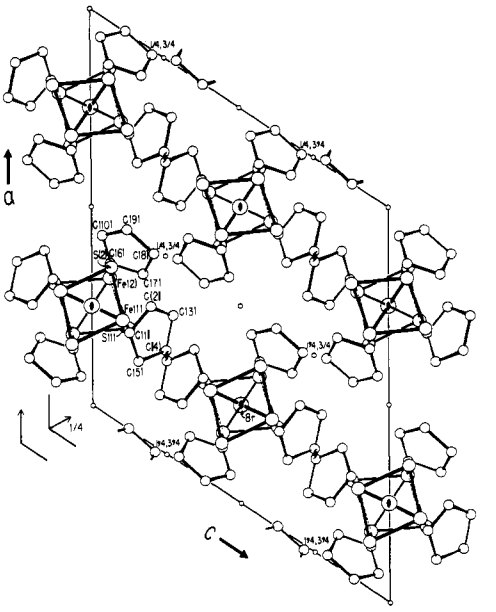

Figure 2. [010] projection showing the four $[Fe_4(\eta^5\text{-}C_5H_5)_4(\mu_3\text{-}S)_4]^+$ monocations and four bromide anions each lying on a crystallographic twofold axis in the monoclinic unit cell of $A2/a$ symmetry.

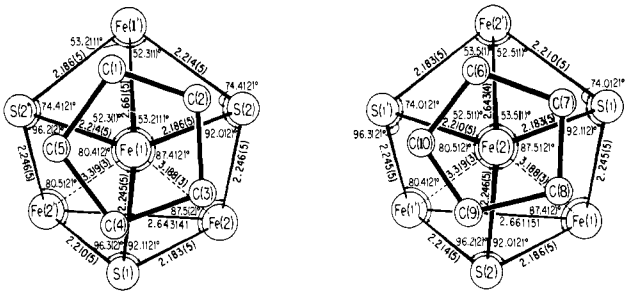

Figure 3. Local environment about each of the two crystallographically independent iron atoms showing the essential equivalence of these two atoms.

possesses a d^5 Fe(III) configuration. The metal cluster model assumes[20] that two of the five 3d iron AO's are essentially nonbonding with respect to direct tetrairon interactions in their being primarily involved in bonding with cyclopentadienyl ring orbitals. More specifically, the $(e + t_1 + t_2)$ iron symmetry orbitals, constructed under T_d symmetry for these two 3d AO's per iron, may be reasonably assumed to interact principally with the *lower* energy $(e + t_1 + t_2)$ cyclopentadienyl symmetry

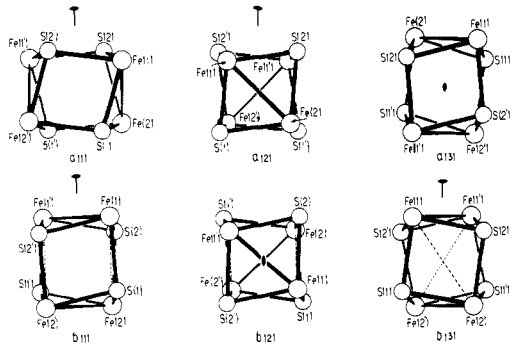

Figure 4. Projections of the Fe_4S_4 framework of (a) the $Fe_4(\eta^5\text{-}C_5H_5)_4(\mu_3\text{-}S)_4$ molecule (with idealized tetragonal D_{2d}-$42m$ geometry) and (b) the $[Fe_4(\eta^5\text{-}C_5H_5)_4(\mu_3\text{-}S)_4]^+$ monocation (with idealized orthorhombic D_2-222 geometry) viewed down the same three orthogonal principal symmetry directions. For the neutral molecule a(2) corresponds to the view down the S_4-$\bar{4}$ axis (which contains two vertical σ_d mirror planes at right angles to each other along the Fe–Fe bonds), while a(1) and a(3) correspond to views down the two symmetry related molecular C_2-2 axes. For the monocation b(1), b(2), and b(3) correspond to views down the three molecular C_2-2 axes. In each species, the direction of the *crystallographic* twofold axis is indicated for each view.

orbitals (arising from the filled, localized e_1-type orbitals of each cyclopentadienyl ring) to give *filled* Fe–C_5H_5 ($e + t_1 + t_2$) *bonding* combinations (mainly of C_5H_5 orbital character) and *empty* Fe–C_5H_5 ($e + t_1 + t_2$) *antibonding* combinations (principally of iron 3d orbital character). Since the other three 3d iron AO's, which are strongly involved in direct Fe–Fe interactions, produce under T_d symmetry six *bonding* ($a_1 + e + t_2$) tetrairon levels and six corresponding antibonding ($t_1 + t_2$) tetrairon levels, the 20 available electrons from the four Fe(III) are distributed among the 20 3d iron symmetry orbitals in accord with the electronic configuration $(a_1 + e + t_2)^{12}(t_1 + t_2)^8(e + t_1 + t_2)^0$ under T_d symmetry. Such a 20-electron system is predicted to distort via a first-order Jahn–Teller effect to give a tetragonal D_{2d} geometry containing a distorted iron tetrahedron. The observed geometry for the $Fe_4(\eta^5\text{-}C_5H_5)_4(\mu_3\text{-}S)_4$ molecule with two short bonding and four long nonbonding Fe–Fe distances provides definite evidence that the LUMO is a doubly degenerate e orbital which is strongly antibonding between the two pairs of bonding iron atoms.

Upon removal of one valence electron from the neutral $Fe_4(\eta^5\text{-}C_5H_5)_4(\mu_3\text{-}S)_4$ to form the oxidized monocation, the observed deformation from a D_{2d} molecular geometry to a D_2 geometry may also be rationalized by the first-order Jahn–Teller theorem if the remaining unpaired electron resides in the degenerate e level (under D_{2d} symmetry). In this case the degenerate e orbitals are split under D_2 symmetry into a ($b_2 + b_3$) orbital set. Furthermore, since molecular deformations are restricted to those configurations which are vibronically allowed,[21] in order to understand the stretching mode symmetry a qualitative normal mode analysis was considered on the basis of the six localized Fe–Fe interactions of the $Fe_4(\eta^5\text{-}C_5H_5)_4(\mu_3\text{-}S)_4$ molecule along the six edges of the deformed iron tetrahedron corresponding to the six internal displacement coordinates[22] under D_{2d} point group symmetry. This examination indicates that the stretching of the two Fe–Fe bonds perpendicular to the principal S_4 axis are of an e mode, while the stretchings involving the four remaining Fe–Fe localized bonds are of ($a_2 + b_2 + e$) modes with the b_2 mode being symmetric and the a_2 mode being antisymmetric with respect to the two vertical σ_d mirrors. The tetrairon framework should be deformed in the same fashion—that is, depending upon which antibonding iron symmetry orbitals are populated, either the two Fe–Fe bonds perpendicular to the principal axis or the other four Fe–Fe bonds should be lengthened. Hence, the observed D_{2d} geometry of the neutral $Fe_4(\eta^5\text{-}C_5H_5)_4(\mu_3\text{-}S)_4$ with the two *bonding* Fe–Fe distances perpendicular to the principal S_4 axis is in accord with the two unoccupied antibonding tetrairon orbitals being of a degenerate e type and with the four filled antibonding tetrairon orbitals of ($a_2 + b_2 + e$) representations. Since the filled *degenerate* e orbitals of $Fe_4(\eta^5\text{-}C_5H_5)_4(\mu_3\text{-}S)_4$ have the same symmetry as the e stretching mode, when an electron is removed from these e orbitals to form the monocation, the degeneracy is removed such that the four formerly equivalent nonbonding Fe–Fe distances become *nonequivalent* in two distinct pairs as observed in the $[Fe_4(\eta^5\text{-}C_5H_5)_4(\mu_3\text{-}S)_4]^+$ species.

It is noteworthy that an Fe–Fe distance of 2.925 (4) Å was found[23] in the pseudobioctahedral edge-bridged $[cis\text{-}Fe_2(\eta^5\text{-}C_5H_5)_2(CO)_2(\mu_2\text{-}SR)_2]^+$ monocation (R = C_2H_5) compared to the corresponding nonbonding value of 3.39 Å determined[24] in the neutral diphenylmercapto homologue. This greatly decreased Fe–Fe distance of 0.47 Å in the Fe_2S_2 core of the dimeric monocation was interpreted[23] in terms of the removal by oxidation of an electron of predominantly antibonding iron character to give (in simple valence bond language) a localized total metal–metal bond order of 0.5. The significant decrease by 0.2 Å of only two of the four nonbonding distances in the $[Fe_4(\eta^5\text{-}C_5H_5)_4(\mu_3\text{-}S)_4]^+$ monocation would likewise correlate (to a first approximation) to each of these two Fe–Fe interactions increasing its metal–metal bond order from *zero* to 0.25. This interpretation is based upon the two short (and unaffected) Fe–Fe distances in the monocharged tetramer still representing electron-pair bonds (each of bond order 1.0) and the two longest Fe–Fe distances still conforming to the bond order of *zero*. The total limiting Fe–Fe bond order of 2.5 is in accord with the 12 bonding and 7 antibonding electrons associated with the direct tetrairon interactions in the monocation. This description of individual metal–metal bond orders involving localization of the antibonding electrons between certain pairs of iron atoms, as estimated from the determined differences in Fe–Fe distances, is founded on an arbitrary judgment; the application of the qualitative MO metal cluster model to the $[Fe_4(\eta^5\text{-}C_5H_5)_4(\mu_3\text{-}S)_4]^+$ monocation does not restrict the extent of electron delocalization within the tetrairon cluster orbitals in that it provides only the total limiting Fe–Fe bond order of 2.5.

In the cubane-like organometallic compound family, the $[Fe_4(\eta^5\text{-}C_5H_5)_4(\mu_3\text{-}S)_4]^n$ (n = 0, +1) complexes are intermediate cases between a completely bonding and a completely nonbonding tetrahedron in that the antibonding metal cluster orbitals (t_1 and t_2 under T_d symmetry) are partially occupied. It is in these intermediate cases where the first-order Jahn–Teller effect may be operational to induce the geometrical deviations from T_d symmetry of the metal framework; the resulting subgroup geometries are functions of the number of the metal cluster antibonding electrons. When all of the metal cluster antibonding t_1 and t_2 orbitals are filled, such as in the cases of $Co_4(CO)_{12}(\mu_3\text{-}Sb)_4$,[25] $Os_4(CO)_{12}(\mu_3\text{-}O)_4$,[26] $Re_4(CO)_{12}(\mu_3\text{-}SCH_3)_4$,[27] and $Pt_4(CH_3)_{12}(\mu_3\text{-}X)_4$ (X = OH, Cl, I),[28] an idealized T_d metal tetrahedron is conserved (in the assumed absence of distortions due to steric pressures[4a,b]) from electronic considerations with no net metal–metal bonding, as reflected by the nonbonding metal–metal distances observed in these tetramers.[29] A T_d metal configuration may be also conserved electronically when all of the metal cluster antibonding orbitals are empty and the bonding ones are filled such as in the case of $Fe_4(\eta^5\text{-}C_5H_5)_4(\mu_3\text{-}CO)_4$[19] which has been shown to possess a completely bonding metal tetrahedron with six chemically equivalent metal–metal distances in the electron-pair bonding range.

Further synthetic and structural investigations of other cubane-like metal clusters are in progress in order to determine and thereby systematize the deviations of metal tetrahedra from T_d symmetry for all molecular orbital-electronic con-

figurations where the number of electrons involved in the *direct* metal–metal interactions ranges from 13 to 23.

Acknowledgments. We are very appreciative for the financial support rendered by the National Science Foundation (No. GP-42309X) for this investigation. The use of the UNIVAC 1110 computer at the Academic Computing Center, University of Wisconsin (Madison), was made available through partial support of the National Science Foundation, administered through the University Research Committee. Special thanks are given to Dr. Phillip J. Vergamini at Wisconsin (now at University of California, Los Alamos Scientific Laboratory) for helpful consultations.

Supplementary Material Available: Table III containing equations of least-squares planes for the cyclopentadienyl rings and Table IV containing observed and calculated structure factors (9 pages). Ordering information is given on any current masthead page.

References and Notes

(1) Presented in part at the 161st National Meeting of the American Chemical Society, Los Angeles, Calif., March 1971; based in part upon a dissertation submitted by Trinh-Toan to the Graduate School of the University of Wisconsin (Madison) in partial fulfillment of the requirements for the Ph.D. degree, Jan. 1972.
(2) Author to whom correspondence should be addressed.
(3) Trinh-Toan, W. P. Fehlhammer, and L. F. Dahl, *J. Am. Chem. Soc.*, **94,** 3389 (1972).
(4) (a) G. L. Simon and L. F. Dahl, *J. Am. Chem. Soc.*, **95,** 2164, 2175 (1973); (b) R. S. Gall, N. G. Connelly, and L. F. Dahl, *ibid.*, **96,** 4017 (1974); (c) R. S. Gall, C. Ting-Wah Chu, and L. F. Dahl, *ibid.*, **96,** 4019 (1974).
(5) J. A. Ferguson and T. J. Meyer, *Chem. Commun.*, 623 (1971).
(6) (a) R. A. Schunn, C. J. Fritchie, Jr., and C. T. Prewitt, *Inorg. Chem.*, **5,** 892 (1966); (b) C. H. Wei, R. G. Wilkes, P. M. Treichel, and L. F. Dahl, *ibid.*, **5,** 900 (1966).
(7) W. D. Phillips, M. Poe, C. C. McDonald, and R. B. Bartsch, *Proc. Natl. Acad. Sci. U.S.A.*, **67,** 682 (1970).
(8) It was subsequently shown[9] that the Fe_4S_4 cores in the $[Fe_4(SR)_4(\mu_3\text{-}S)_4]^n$ ($n = -1, -2, -3$) series rather than in the $[Fe_4(\eta^5\text{-}C_5h_5)_4(\mu_3\text{-}S)_4]^n$ series are suitable analogues to the corresponding Fe_4S_4 cores in the *Chromatium* high-potential iron protein and the bacterial ferredoxin from *Micrococcus aerogenes*.[10]
(9) (a) T. Herskovitz, B. A. Averill, R. H. Holm, J. A. Ibers, W. D. Phillips, and J. F. Weiher, *Proc. Natl. Acad. Sci. U.S.A.*, **69,** 2437 (1972); (b) B. A. Averill, T. Herskovitz, R. H. Holm, and J. A. Ibers, *J. Am. Chem. Soc.*, **95,** 3523 (1973); (c) L. Que, Jr., M. A. Bobrik, J. A. Ibers, and R. H. Holm, *ibid.*, **96,** 4168 (1974).
(10) (a) C. W. Carter, Jr., S. T. Freer, Ng. H. Xuong, R. A. Alden, and J. Kraut, *Cold Spring Harbor Symp. Quant. Biol.*, **36,** 381 (1971); (b) L. C. Sieker, E. T. Adman, and L. H. Jensen, *Nature (London)*, **235,** 40 (1972); (c) C. W. Carter, Jr., J. Kraut, S. T. Freer, R. A. Alden, L. C. Sieker, E. T. Adman, and L. H. Jensen *Proc. Natl. Acad. Sci. U.S.A.*, **69,** 3526 (1972); (d) E. T. Adman, L. C. Sieker, and L. H. Jensen, *J. Biol. Chem.*, **248,** 3987 (1973); (e) C. W. Carter, Jr., J. Kraut, S. T. Freer, and R. A. Alden, *J. Biol. Chem.*, **249,** 6339 (1974); (f) L. H. Jensen, *Annu. Rev. Biochem.*, **43,** 461 (1974); (g) S. T. Freer, R. A. Alden, C. W. Carter, Jr., and J. Kraut, *J. Biol. Chem.*, **250,** 46 (1975).
(11) All analyses were performed by Gailbraith Laboratories, Inc., Knoxville, Tenn. 37921.
(12) Trinh-Toan and L. F. Dahl, *J. Am. Chem. Soc.*, **93,** 2654 (1971).
(13) Calculations were performed on a UNIVAC 1110 computer. Programs used included original or modified versions of (a) A. S. Foust, ANGSET, Ph.D. Thesis (Appendix), University of Wisconsin-Madison, 1970; (b) E. F. Epstein, DREDGE, University of Wisconsin-Madison; (c) J. F. Blount, DEAR, an absorption correction program based on the method of W. R. Busing and H. A. Levy, *Acta Crystallogr.*, **10,** 180 (1957); (d) J. F. Blount, FOURIER, Ph.D Thesis (Appendix), University of Wisconsin-Madison, 1965; (e) W. R. Busing, K. O. Martin, and H. A. Levy, ORFLS, ORNL-TM-305, Oak Ridge National Laboratory, 1962; (f) W. R. Busing, K. O. Martin, and H. A. Levy, ORFFE, ORNL-TM-306, Oak Ridge National Laboratory, 1964; (g) J. C. Calabrese, MIRAGE, Ph.D. Thesis (Appendix), University of Wisconsin-Madison, 1971; (h) D. L. Smith, PLANES, Ph.D. Thesis (Appendix), University of Wisconsin-Madison, 1962.
(14) V. A. Uchtman and L. F. Dahl, *J. Am. Chem. Soc.*, **91,** 3756 (1969).
(15) "International Tables for X-Ray Crystallography", Vol. III, The Kynoch Press, Birmingham, England, 1962: (a) p 157; (b) p 215.
(16) $R_1 = [\Sigma||F_o| - |F_c||/\Sigma|F_o|] \times 100$ and $R_2 = [\Sigma w_i||F_o| - |F_c||^2/\Sigma w_i|F_o|^2]^{1/2} \times 100$. All least-squares refinements were based on the minimization of $\Sigma w_i||F_o| - |F_c||^2$ with the individual weights $w_i = 1/\sigma(F_o)^2$.
(17) Atomic scattering factors used for all atoms except hydrogen are from H. P. Hanson, F. Herman, J. D. Lea, and S. Skillman, *Acta Crystallogr.*, **17,** 1040 (1964); those for the hydrogen atoms are from R. F. Stewart, E. R. Davidson, and W. T. Simpson, *J. Chem. Phys.*, **42,** 3175 (1965). Real and imaginary corrections for anomalous dispersion for Mo Kα radiation were applied in the final least-squares cycles for the Br and Fe atoms (i.e., $\Delta f' = -0.3$ and $\Delta f'' = 2.6$ for Br; $\Delta f' = 0.4$ and $\Delta f'' = 1.0$ for Fe).[15b]
(18) L. Pauling, "The Nature of the Chemical Bond", 3d ed, Cornell University Press, Ithaca, N.Y., 1960, p 260.
(19) M. A. Neuman, Trinh-Toan, and L. F. Dahl, *J. Am. Chem. Soc.*, **94,** 3383 (1972).
(20) Trinh-Toan, B. K. Teo, J. A. Ferguson, T. J. Meyer, and L. F. Dahl, *J. Am. Chem. Soc.* following paper in this issue.
(21) R. W. Jotham and S. F. A. Kettle, *Inorg. Chim. Acta*, **5,** 183 (1971).
(22) (a) E. B. Wilson, Jr., J. C. Decius, and P. C. Cross, "Molecular Vibrations", McGraw-Hill, New York, N.Y., 1955; (b) F. A. Cotton, "Chemical Applications of Group Theory", 2d ed, Wiley-Interscience, New York, N.Y., 1971.
(23) N. G. Connelly and L. F. Dahl, *J. Am. Chem. Soc.*, **92,** 7472 (1970).
(24) G. Ferguson, C. Hannaway, and K. M. S. Islam, *Chem. Commun.*, 1165 (1968).
(25) A. S. Foust and L. F. Dahl, *J. Am. Chem. Soc.*, **92,** 7337 (1970).
(26) D. Bright, *Chem. Commun.*, 1169 (1970).
(27) E. W. Abel, W. Harrison, R. A. N. McLean, W. C. Marsh, and J. Trotter, *Chem. Commun.*, 1531 (1970); W. Harrison, W. C. Marsh, and J. Trotter, *J. Chem. Soc., Dalton Trans.*, 1009 (1972).
(28) R. N. Hargreaves and M. R. Truter, *J. Chem. Soc., A*, 90 (1971), and references cited therein.
(29) The fact that considerable nonsystematic variations in metal–metal distances have been found in the solid state for cubane-like tetramers containing a nonbonding tetrahedron of metal atoms has been attributed to anisotropic steric effects which are expected from potential energy considerations to produce a maximum variation in metal–metal distances for which the interactions are nonbonding.[4a,b] Our metal cluster model assumes the presence of only sterically innocent ligands.